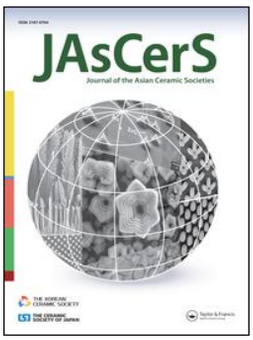

Journal of Asian Ceramic Societies

ISSN: (Print) 2187-0764 (Online) Journal homepage: https://www.tandfonline.com/loi/tace20

Microstructure and mechanical, physical and structural properties of sustainable lightweight metakaolin-based geopolymer cements and mortars employing rice husk

Hamed I. Riyap, Christelle N. Bewa, Charles Banenzoué, Hervé K. Tchakouté, Claus H. Rüscher, Elie Kamseu, Maria C. Bignozzi & Cristina Leonelli

To cite this article: Hamed I. Riyap, Christelle N. Bewa, Charles Banenzoué, Hervé K. Tchakouté, Claus H. Rüscher, Elie Kamseu, Maria C. Bignozzi & Cristina Leonelli (2019): Microstructure and mechanical, physical and structural properties of sustainable lightweight metakaolin-based geopolymer cements and mortars employing rice husk, Journal of Asian Ceramic Societies, DOI: 10.1080/21870764.2019.1606140

To link to this article: https://doi.org/10.1080/21870764.2019.1606140

Accepted author version posted online: 15 Apr 2019.
Published online: 22 Apr 2019.

JOURNAL OF ASIAN CERAMIC SOCIETIES
https://doi.org/10.1080/21870764.2019.1606140

THE CERAMIC SOCIETY OF JAPAN
THE KOREAN CERAMIC SOCIETY
Taylor & Francis
Taylor & Francis Group

ARTICLE

Microstructure and mechanical, physical and structural properties of sustainable lightweight metakaolin-based geopolymer cements and mortars employing rice husk

Hamed I. Riyap[a], Christelle N. Bewa[a], Charles Banenzoué[b], Hervé K. Tchakouté[a,c], Claus H. Rüscher[c], Elie Kamseu[d,e], Maria C. Bignozzi[f] and Cristina Leonelli[e]

[a]Laboratory of Applied Inorganic Chemistry, Faculty of Science, Department of Inorganic Chemistry, University of Yaounde I, Yaounde, Cameroon; [b]Faculty of Science, The University of Douala, Douala, Cameroon; [c]Institut für Mineralogie, Leibniz Universität Hannover, Hannover, Germany; [d]Department of Research, Local Materials Promotion Authority, Yaounde, Cameroon; [e]Department of Engineering "Enzo Ferrari", University of Modena and Reggio Emilia, Modena, Italy; [f]Department of Civil Engineering, Chemistry, Environmental and Materials, University of Bologna, Bologna, Italy

ABSTRACT

This work focuses on an in-depth investigation of the formation of pores in the structure of lightweight geopolymer cements and mortars using rice husk as a foaming agent. The hardener used in this study was sodium waterglass. Metakaolin was replaced by 0, 10, 20, 30 and 40 % by mass of husk and the obtained powders were used to produce lightweight geopolymer cements and mortars. The formation of pores in the lightweight geopolymer cements was monitored using X-ray diffractometry and infrared spectroscopy while those in the mortars were assessed using apparent density and compressive strength measurements, mercury intrusion porosimetry and optical and scanning electron microscopy. The values for the compressive strength and apparent density were in the ranges of 28.92–0.75 MPa and 1.88–1.70 g/cm^3, respectively. The results indicated that the values for the compressive strength and apparent density of geopolymer mortars decreased while those of the cumulative pore volume increased with increases in the metakaolin replacement level. Stereomicroscopic and scanning electron microscopic images showed the presence of rice husk and fibres of rice husk, respectively, in the networks. It was found that rice husk can be used as a foaming agent for producing sustainable lightweight geopolymer mortars.

ARTICLE HISTORY
Received 22 November 2018
Accepted 13 March 2019

KEYWORDS
Rice husk; metakaolin; hardener; lightweight geopolymers; compressive strength

1. Introduction

Porous or lightweight materials have been used as purification membranes, high-efficiency adsorption materials, catalysts or building materials for thermal insulation and acoustic materials [1]. These materials can be prepared using organic polymers (extruded polystyrene, expanded polystyrene, etc.) and inorganic chemical reagents (aluminum powders, H_2O_2, sodium perborate, silica fume, CaC_2, O_2, etc.). These foaming agents create macropores in the structure of the final products. Alghamdi and Neithalath [2] activated fly ash using sodium carbonate as a foaming agent for producing lightweight geopolymer matrices. These foaming agents are expensive, however, and their production is energy intensive and emits greenhouse gases into the atmosphere. In order to alleviate these drawbacks, some researchers such as Ngouloure et al. [3] have used waste materials as foaming agents for producing lightweight geopolymer cements which employ recycled natural waste products such as rice husk ash and volcanic ash as foaming agents to prepare metakaolin-based porous geopolymers for insulating applications. Fongang et al. [4] used sawdust as a foaming agent to produce lightweight insulating composites. Yahya et al. [5] used rice husk as an additive in fly ash-based geopolymer mortars. These authors investigated the effects of rice husk on the properties of fly ash-based geopolymer mortars using compressive strength, density and water absorption. They concluded that the values of the densities of the samples indicated that rice husk can be used to produce lightweight geopolymer concretes. The production of rice generates immense volumes of rice husk because rice is one of the world's major food crops. In Cameroon, more rice is produced in the West Highlands (North-West and West regions), North region (North and Far North regions). But some researchers such as Tchakouté et al. [6–8] and Kamseu et al. [9] burned this waste and used the rice husk ash obtained to produce sustainable sodium waterglass. For use in preparing geopolymer cements. Melele et al. [10] used sodium waterglass from rice husk ash to enhance the reactivity of soda lime silica glass solutions. Mabah et al. [11] and Tchuente et al. [12] also used rice husk ash to produce cleaner semi-crystalline and amorphous calcium silicate, respectively, as

CONTACT Hervé K. Tchakouté htchak@yahoo.fr

additives to alter the microstructures of the geopolymer cements. It is important to indicate that the Upper Nyoung Valley Development Association (UNVDA) in the North-West of Cameroon produces about one ton of rice husk per day in nature [13–15]. Up to the present, no initiative has been planned by the government or private companies to promote this waste. In order to leverage the value of this waste material, we propose using rice husk as a foaming agent for producing geopolymer mortars.

In order to conduct an in-depth investigation into the formation of pores in the structure of lightweight geopolymer mortars using a natural foaming agent such as rice husk, metakaolin was replaced by 0, 10, 20, 30 and 40 % by mass of rice husk. The resultant powders were used to study the influence of low-cost rice husk as a foaming agent on the properties of lightweight geopolymer cements and mortars. The structural properties of lightweight geopolymer cements were studied using X-ray diffractometry and infrared spectroscopy in order to appreciate the behaviour of the binder and the formation of pores in the network when metakaolin is replaced by rice husk. The microstructure was measured by such methods as stereomicroscopy, scanning electron microscopy and mercury intrusion porosimetry of geopolymer mortars. The mechanical and physical properties of geopolymer mortars such as their compressive strength and apparent density respectively were also evaluated.

2. Materials and geological setting

2.1. Materials

The kaolin used in this study was extracted from Dibamba in the Littoral region of Cameroon. The rice husk (RH) was collected by the Upper Nyoung Valley Development Association (UNVDA) in Ndop, Department of Ngoketundjia, a region in the North-West (Cameroon). The kaolin was ground for 30 min into fine powders using a rapid ball mill (MGS Sarl) with a porcelain jar and microspheres of high-grade alumina as a grinding medium. The obtained powders of kaolin (Dib_0) were calcined in a programmable electric furnace (MGS Sarl) for 4 h at a heating and cooling rate of 5 °C/min at 700 °C to obtain metakaolin ($MK\text{-}Dib_0$). It is important to note that the kaolin used in this study had already been used by Tchakouté et al. [8,13] in the production of geopolymer cements. The authors reported that this kaolin contained kaolinite, illite, quartz, and anatase. NaOH pellets, a commercial product marketed by Merck (KGaA, 64271 Darmstadt, Germany, with 99% purity) were used as the Na_2O source. The commercial sodium silicate solution used in this study was provided by Ingessil Srl Verona (Italy). It's chemical composition was 14.37 wt% Na_2O, 29.54 wt % SiO_2, 56.09 wt% H_2O. The aggregate used in this study was river sand collected from Cameroon's Sanaga River with large particles passed through a 1250 µm mesh. The chemical compositions of kaolin and Sanaga River sand are shown in Table 1 and the X-ray pattern of the

Table 1. Chemical compositions of kaolin (Dib_0) and sand %wt.

Sample / Oxides	Dib_0 [8, 13]	Sand
MgO	0.20	/
Al_2O_3	33.90	5.00
SiO_2	47.10	89.00
P_2O_5	0.034	/
SO_3	< 0.02	/
K_2O	0.42	
Na_2O	< 0.10	3.52
CaO	0.21	
TiO_2	0.83	/
Cr_2O_3	/	/
Fe_2O_3	0.99	0.92
ZnO	/	/
SrO	/	/
ZrO_2	/	/
LOI	14.75	1.56

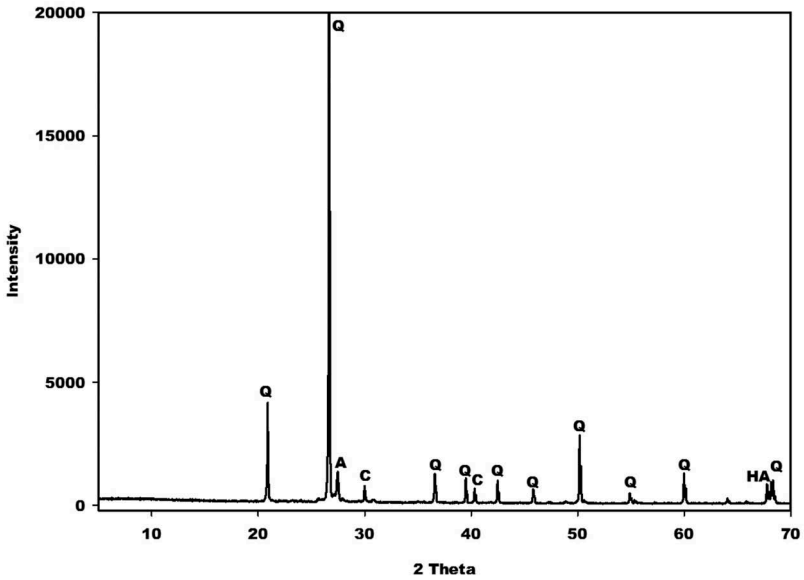

Figure 1. X-ray pattern of Sanaga river sand. Q, A, C and HA denote peaks of quartz, albite, calcite and halite, respectively.

sand is showing in Figure 1. The X-ray pattern of the sand shows some reflection peaks of quartz, albite, calcite and halite.

2.2. Geological setting

The study area of Dibamba kaolin from Tertiary formation is located in the Douala sub-basin between 9° 45′ and 9° 50′ East longitude and 4° 02′ and 4° 05′ North latitude. The Douala sub-basin is located in the Gulf of Guinea between the Cameroon volcanic Line to the north and the Kribi-Campo sub-basin to the south [16]. Dibamba kaolin is embedded in Dibamba sandstone deposits which are 1.5–3 m thick. The Dibamba sandstone deposit occurs as layers of yellowish, pinkish, reddish and whitish sandstones measuring 1 mm to a few centimetres thick. The embedded kaolin occurs as whitish layers (5–10 cm thick) and nodules, with have a soapy feel. The whitish layers are found between two reddish sandstone layers, whereas the nodules are surrounded by yellowish or pinkish layers. In some parts of the outcrops, the different laminate and layers of sandstones are deposited in a cross-bedding structure [17].

3. Methods and experimental procedures

3.1. Preparation of the hardener

The hardener was prepared by adding sodium hydroxide pellets to commercial sodium silicate. The whole was mixed with distilled water in order to obtain chemical reagents with SiO_2/Na_2O and H_2O/Na_2O molar ratios equal to 1.5 and 10, respectively. The chemical reagent thus obtained was stored at ambient temperature for at least one week before use in order to allow full depolymerization of the bridging oxygen (-Si-O-Si-) contained in the commercial sodium waterglass.

3.2. Synthesis of geopolymer cements and mortars

Geopolymer cements were prepared by gradually adding the prepared chemical ingredient to metakaolin with various proportions of rice husk (metakaolin replacement levels 0, 10, 20, 30 and 40 % by mass) in a porcelain mortar and mixed mechanically for 5 min. One part of each slurry was cast in cylindrical moulds (20 × 10 mm). Another part was mixed with river sand using a set mass binder/sand ratio of 1:3 and mixed mechanically for about 5 min. The mass binder/sand ratio of 1:3 was chosen according to the findings of a study by Liu et al. [18]. The mortars obtained were cast in cubic moulds (40 × 40 × 40 mm) and rectangular moulds (40 × 40 × 15 mm). The moulded geopolymer cements and mortars were covered with plastic and kept for 24 h at the ambient temperature in the laboratory before demoulding. The specimens obtained were demoulded after 24 h and sealed in the plastic for 28 days at 26 ± 2 °C and 60 % humidity. The geopolymer cements containing 0, 10, 20, 30 and 40 % by mass of rice husk were labelled GPC0, GPC10, GPC20, GPC30 and GPC40, respectively, and the corresponding mortars were labelled MGPC0, MGPC10, MGPC20, MGPC30 and MGP40, respectively.

3.3. Methods of characterization of raw materials, geopolymer cements and mortars

Measurements of the chemical composition of the Sanaga river sand were carried out by X-ray fluorescence (XRF) using a Bruker S4 PIONEER with a wavelengths dispersive (WD-XRF) spectrometer).

The influence of the rice husk on the mechanical and microstructural properties of the final products was evaluated by measuring the compressive strengths

of the geopolymer mortars from the sample moulded in the 40 × 40 × 40 mm cubic moulds after 28 days with an automatic hydraulic press (Impact Test Equipment Limited, Building 21, Stevenston Industrial Estate, Stevenston, Ayrshire, Scotland, UK KA20 3LR) with a 250 kN capacity and loading rate of 0.500 MPa/s meeting the EN196/01 standard. After the compressive strength test, fragments of the selected compositions were used for SEM analysis and each composition was observed using an optical microscope apparatus.

The lightweight geopolymer cements moulded in 20 × 10 mm cylindrical moulds at room temperature were crushed after 28 days and the powders obtained were used for XRD and infrared spectroscopy measurement. XRD patterns of rice hush, metakaolin and geopolymer cements were taken using CuKα radiation between 5° and 80° (2θ) for 7 h in 0.03° steps using a Bruker D4. The IR absorption spectra were taken by the KBr method (200 mg KBr, 1 mg sample, Bruker Vertex 80 v, 2 cm^{-1}, 32 scans).

Fragments of the lightweight geopolymer mortars from the mechanical testing of each composition were used for optical microscopic observation with a video stereomicroscope (Ceramic Instrument Model 101T-M7) equipped with a binocular head and Tablet 7″ with integrated 2 MP micro camera. This system enables observation with a direct Vision Eyepieces directly in the monitor. Other selected fragments of geopolymer mortars and rice husk after gold-coating and drying were employed for microstructure observation using a JEOL JSM-6390A Scanning Electron Microscope (SEM) with an acceleration voltage of 30.0 kV.

Selected MGP0, MGP20 and MGP40 fragments collected from the mechanical test with the volume of about 1 cm^3 were used to prepare specimens for Mercury Intrusion Porosimeter (MIP) tests. The dried samples were put in a penetrometer with a 15 mL sample cup and a steam volume of 0.38 mL. The pore size distribution measurements were carried out with a MIP (Autopore IV 9500, Micromeritics). Porosity was evaluated using the set-time equilibrium (10 sec) mode between pressure limits of 345 kPa and 228 MPa. Under these operating conditions, it was possible to measure capillary pores across a wide range (0.006–350 μm).

Lightweight geopolymer mortars moulded in rectangular moulds (40 × 40 × 15 mm) were used for measuring the apparent density without mercury by the Archimedes' method with an automatic densimeter (Ceramic Instrument mod. DDA/2) in accordance with DIN-51097 standards.

4. Results and discussion

4.1. Characterization of the raw materials

4.1.1. X-ray patterns

X-ray patterns of metakaolin (MK-Dib_0) and rice husk (RH) are displayed in Figures 2 and 3, respectively. As can be seen, that the X-ray patterns of the two raw materials indicate a broad hump structure located between 15 and 35° (2θ) for metakaolin and between 10 and 38° (2θ) for rice husk corresponding to the presence of the amorphous phase. Besides these amorphous phases, the X-ray pattern for metakaolin shows some crystalline peaks of illite, quartz and

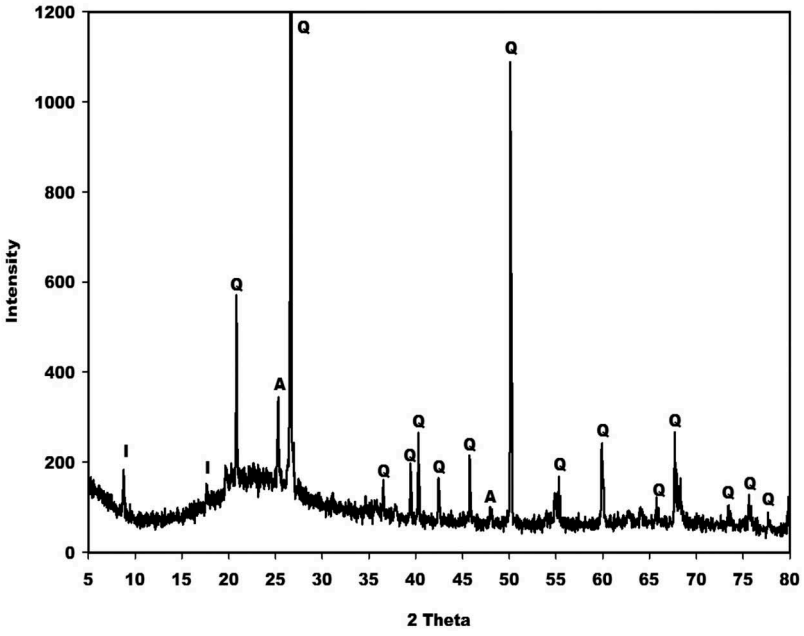

Figure 2. X-ray pattern of metakaolin (MK-Dib0). I, Q and A denote peaks of illite, quartz and anatase, respectively.

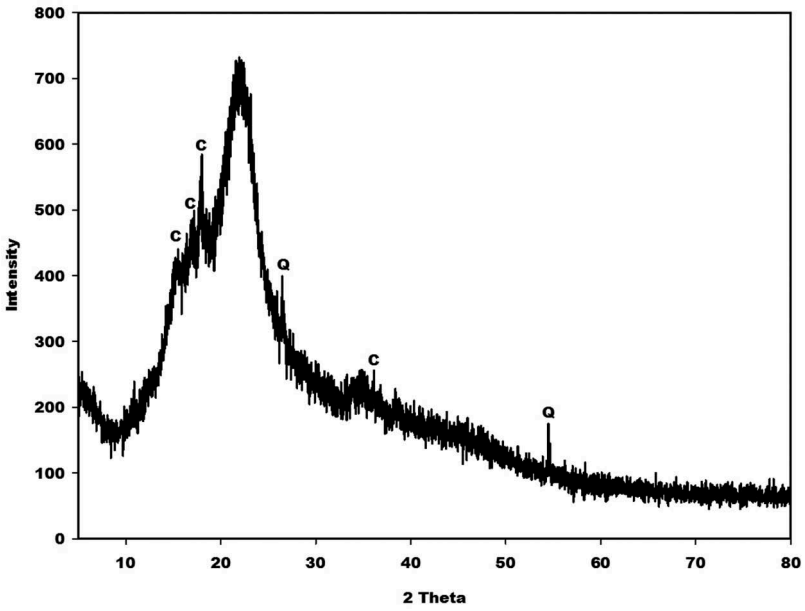

Figure 3. X-ray pattern of rice husk (RH). C and Q denote peaks of cellulose and quartz, respectively.

anatase as impurities, whereas the pattern for rice husk indicates some peaks of quartz and an organic compound such as crystalline cellulose [19–21] as impurities. According to Nakbanpote et al. [22], the presence of this organic compound in the raw material favours the thermal insulation, acoustic, electrical and magnetic properties of the prepared porous materials.

4.1.2. Infrared spectra

The infrared spectra of MK-Dib0 and RH are depicted in Figures 4 and 5, respectively. The absorption bands at 467, 530 and 711 cm^{-1} on the IR spectrum of RH and that at 459 cm^{-1} on the IR spectrum of metakaolin are ascribed to the vibration modes of -Si-O-Si- bonds. Those at 695 and 797 cm^{-1} on the IR spectrum of metakaolin are attributed to vibration modes of Si-O-Si in quartz [19]. The sharp absorption bands observed at about 1080 and 1157 cm^{-1} on the IR spectrum of RH are ascribed to the amorphous and crystalline silica, respectively, in the structure of RH. It is important to note that the band of amorphous silica appears at about 1100 cm^{-1} [23]. The lower wavenumber of this band (1080 cm^{-1}) on the IR spectrum of RH is related to the presence of impurities such as quartz and cellulose in the structure of this waste. This is confirmed by the X-ray pattern of RH (Figure 3). The absorption band at about 1083 cm^{-1} on the IR spectrum of MK-Dib_0 is assigned to the asymmetrical and symmetrical vibration modes of Si-O-Si and Si-O-Al bonds. That at 1037 cm^{-1} on the IR spectrum of RH could be ascribed to the C-O stretching vibration

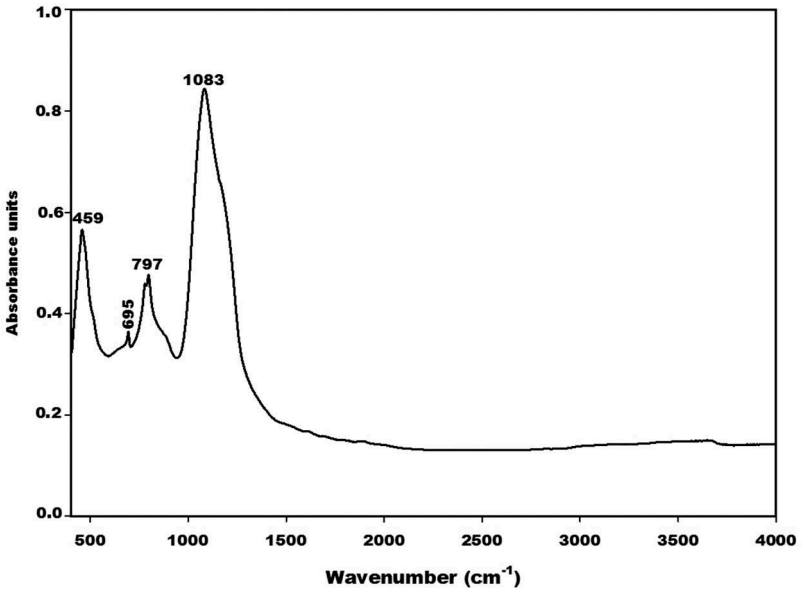

Figure 4. Infrared spectra of metakaolin (MK-Dib0).

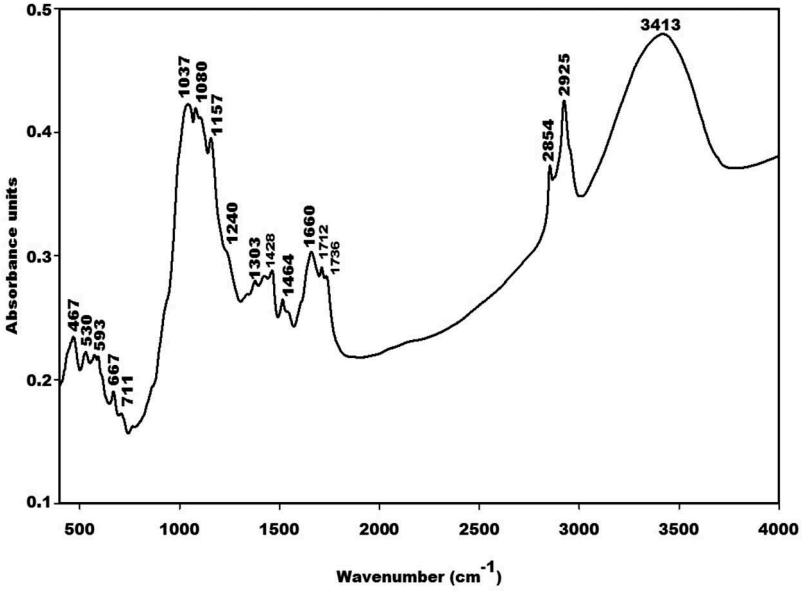

Figure 5. Infrared spectra of rice husk (RH).

modes of cellulose, hemicellulose and lignin [24]. The absorption bands at about 667 and 593 cm^{-1} on the IR spectrum of RH are ascribed to the C-OH vibration modes of polysaccharides [24]. The absorption band at 3413 cm^{-1} corresponds to the stretching vibrations of hydroxyl (-OH) groups of the cellulose and hemicellulose in the structure of RH [25]. Those at 2854 and 2925 cm^{-1} are attributed to the stretching vibration modes of the aliphatic C-H bonds [26–28]. The shoulder band at 1240 cm^{-1} is ascribed to the C-O vibrations of the aryl groups of lignin [29]. The absorption bands at 1736, 1712, 1660, 1464, 1428 and 1303 cm^{-1} are associated with kenotic stretching and carbonyl groups [30,31].

4.1.3. Scanning electron microscopic images coupled with EDX analysis of rice husk

Figure 6 presents a micrograph image and EDX analysis of rice husk (RH). The micrographic image of RH shows some irregular amorphous silica particles distributed unevenly over the full surface of the rice husk. Microanalysis (EDX) of a selected zone of the rice husk indicates that this waste material is composed mainly of silicium (Si), phosphorus (P) associated with potassium (K), magnesium (Mg) and aluminum (Al). This is confirmed by the composition of SiO_2 (32.59 wt.%), P_2O_5 (14.33 wt.%), K_2O (10.02 wt.%), MgO (1.78 wt.%) and Al_2O_3 (1.28 wt.%).

4.2. Structural properties of geopolymer cements

4.2.1. X-ray patterns

X-ray patterns of the selected geopolymer cements are recorded in Figure 7. These spectra indicate a broad hump structure between 18 and 40° (2θ). This hump structure appears at between 15 and 32° (2θ) on the X-ray pattern of metakaolin. The shift of this halo diffraction can be ascribed to the formation of the binder in the network. The shoulder band between 21 and 28° (2θ) on the X-ray patterns of GPC20 and GPC40 geopolymer cements could be associated with unreacted amorphous silica from rice husk. This band is more pronounced on the X-ray pattern of GPC40, thus suggesting that the amount of unreacted amorphous silica increases with increases metakaolin in the replacement level. Some reflection peaks of illite, anatase and quartz are clearly observed in the X-ray patterns of geopolymer cements and metakaolin. This implies that these minerals do not react during the depolymerisation of metakaolin or the polycondensation of the precursors (silicate and aluminate). Besides these minerals, the reflection peaks of cellulose are clearly observed in the X-ray pattern of GPC40.

4.2.2. Infrared spectra

Figure 8 depicts the IR spectra of the selected GPC0, GPC20 and GPC40 geopolymer cements. The absorption bands at 455 and 452 cm^{-1} correspond to the vibration modes of Si-O-Si bonds. Those at 661 and 777 cm^{-1} on the IR spectra of GPC40 are associated with the vibrations of C-OH and Si-O-Si bonds, respectively. These bands appear at 667 and 777 cm^{-1} on the IR spectrum of rice husk. The shift of these absorption bands could be ascribed to the reorganisation of the geopolymer network. The absorption band at 694 cm^{-1} can be attributed to the vibration band of quartz [32,33]. This is consistent with the X-ray patterns of the geopolymer cements, which show the reflection peaks of quartz. The band at around 728 cm^{-1} observed on the IR spectra of GPC0 and GPC20 is assigned to the vibration modes of sialate (Si-O-Al) bonds. This band is not found in the IR spectra of metakaolin or GPC40 geopolymer cement

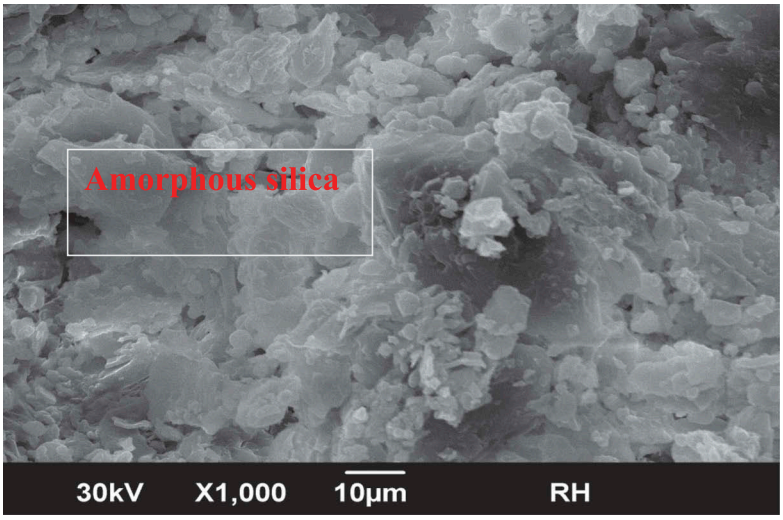

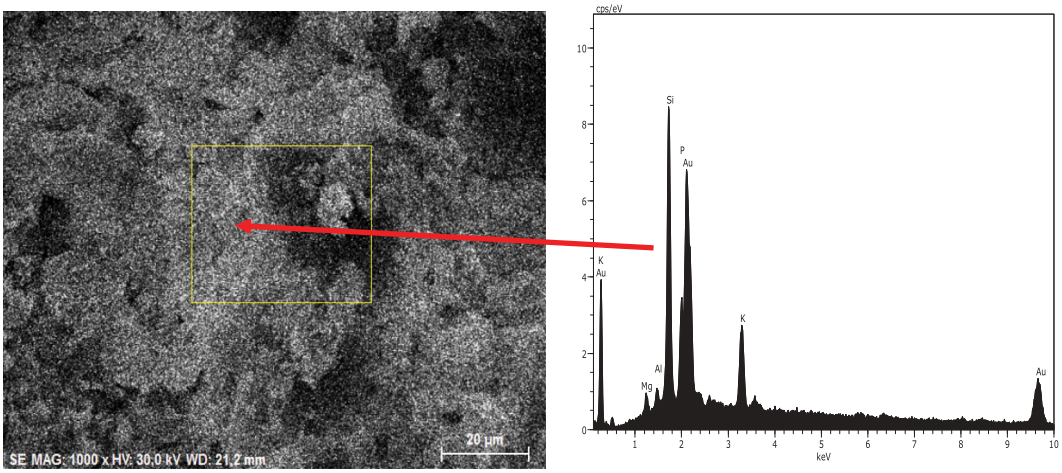

Element	unn. C [wt.%]	norm. C [wt.%]	Atom. C [at.%]	Compound	norm. Comp. C [wt.%]	Error (3 Sigma) [wt.%]
Silizium	5,96	15,23	18,04	SiO2	32,59	0,89
Gold	15,67	40,02	6,76		40,02	1,32
Magnesium	0,42	1,07	1,47	MgO	1,78	0,17
Kalium	3,26	8,31	7,07	K2O	10,02	0,40
Aluminium	0,26	0,68	0,83	Al2O3	1,28	0,13
Phosphor	2,45	6,25	6,71	P2O5	14,33	0,39
Sauerstoff	11,13	28,43	59,12		0,00	9,75
Total:	39,16	100,00	100,00			

Figure 6. Micrograph image and EDX analysis of rice husk (RH).

suggesting the formation of the binder or poly(sialate) bonds (-Si-O-Al-) in the network. It disappears progressively as the metakaolin replacement level increases, indicating a decrease in the amount of binder in the network leading to the formation of pores. The absence of this band on the IR spectrum of GPC40 could be explained by the fact that this system has the lowest amount of binder. The absorption band at about 1019 cm^{-1} in the IR spectra of the selected lightweight geopolymer cements corresponds to the asymmetrical and symmetrical vibration modes of Si-O-M (M: Si, Al). This band appears at 1083 cm^{-1} in the IR spectrum of metakaolin. The shift of this band is associated with the inclusion of Al in the tetrahedral network leading to the formation of a pol(sialate-siloxo) network [34,35]. As can be seen, the wavenumber of this band is the same for all the GPC0, GPC20 and GPC40 geopolymer cements. This suggests that the amorphous silica contained in the structure of rice husk does not incorporate in the poly (sialate-siloxo) network. The absorption band at about 870 cm^{-1} in the IR spectra of GPC0 and GPC20 is ascribed to the silanol (Si-OH) groups. The absence of this band in the IR spectrum of GPC40 indicates the low degree of depolymerisation of the aluminosilicate powder owing to the presence of a greater amount of rice husk in the system. This is confirmed by the incomplete polycondensation reaction leading to the appearance of the absorption bands at around 848 and 1450 cm^{-1}, which are attributed to the vibration

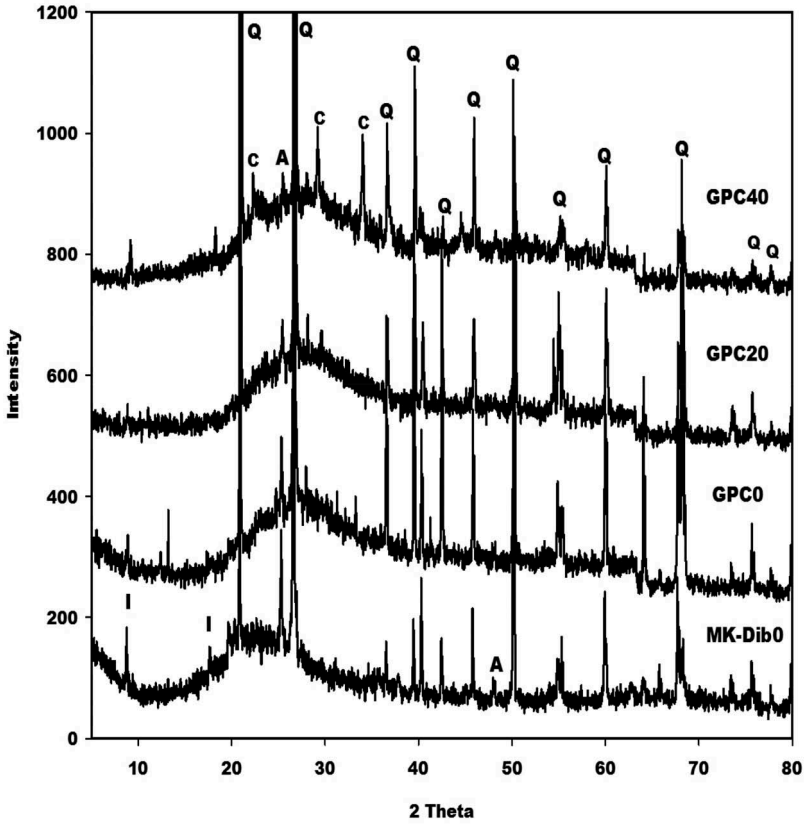

Figure 7. X-ray patterns of metakaolin (MK-Dib0) and geopolymer cements, GPC0, GPC20 and GPC40. I, Q, C and A denote peaks of illite, quartz, cellulose and anatase, respectively.

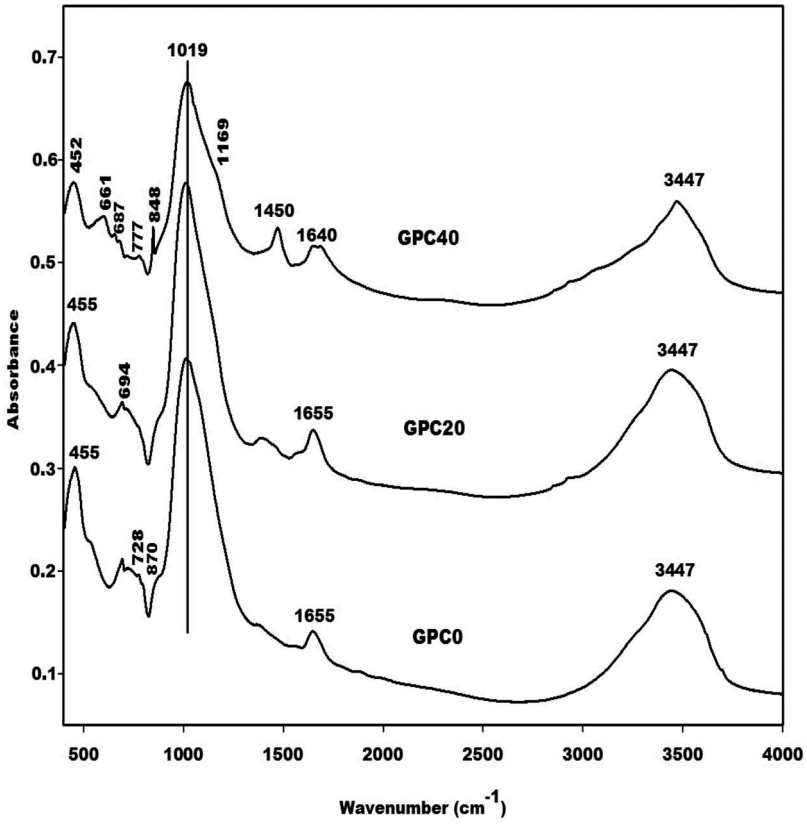

Figure 8. Infrared spectroscopy of geopolymer cements, GPC0, GPC20 and GPC40.

modes of Na_2CO_3. The presence of this band in the IR spectrum of GPC40 could be ascribed to the greater amount of unreacted Na^+ in the network, which reacts to CO_2 in the atmosphere and therefore impedes the polycondensation process. This assessment is justified by the absence of the absorption bands at about 870 and 728 cm^{-1} on the IR spectrum of GPC40. The bands at 1640–1655 and 3447 cm^{-1} belong to the vibration modes of the H-O-H and O-H bonds, respectively, of water molecules.

4.3. Physical and mechanical properties and microstructure of geopolymer mortars

4.3.1. Apparent density

The apparent density of MGPC0, MGPC10, MGPC20, MGPC30 and MGPC40 geopolymer mortars as functions of the replacement level of metakaolin by rice husk are depicted in Figure 9. As can be seen, the values for the apparent densities of MGPC0, MGPC10, MGPC20, MGPC30 and MGPC40 are 1.88, 1.81, 1.78, 1.76 and 1.70 g/cm^3, respectively. It appears that the values for the apparent densities decrease with increases in the replacement of metakaolin (0, 10, 20, 30 and 40% by mass). This could be attributed to a reduction of the binder in the network [5] owing to the replacement of metakaolin by the lightweight additive. This assumption is in agreement with the X-ray patterns of GPC20 and GPC40 geopolymer cements which show a shoulder band of the unreacted amorphous silica from RH as well as the IR spectra of the aforementioned geopolymer cements indicating the progressive disappearance of the absorption band of the poly(sialate) bonds at 728 cm^{-1}. The complete disappearance of this band in the IR spectrum of GPC40 is responsible for giving GPC40 the lowest value for the apparent density. The decrease in the values for the apparent density of geopolymer mortars from 1.88 to 1.70 g/cm^3 suggests that rice husk can be used as an additive for producing lightweight geopolymer cements, mortars and concretes. Despite the decrease in these values, they are still high compared to those obtained by Fongang et al. [4] and Hassan et al. [36]. It is important to note that these authors used sawdust and coconut ash, respectively, as foaming agents. The higher values for the apparent densities of geopolymer cements obtained in this work could be related to the presence of river sand in the matrix.

4.3.2. Compressive strength

The compressive strength of the geopolymer mortars as a function of the percentage of rice husk and the values for compressive strength as a function of the apparent density are clearly shown in Figures 10 and 11, respectively. The values for the compressive strength of MGP0, MGP10, MGP20, MGP30 and MGP40 geopolymer mortars are 28.32, 18.03, 8.53, 3.64 and 0.75 MPa, respectively. It can be seen that the compressive strength decreases with increases in the amount of rice husk added and decrease with decreases in the values for apparent density. This is associated with a reduction in the amount of binder in the network, which contributes to the weakening of the structure of the specimens, suggesting the presence of voids and pores in the system. The decrease in the values for the compressive strength could also be related to unreacted amorphous silica in the

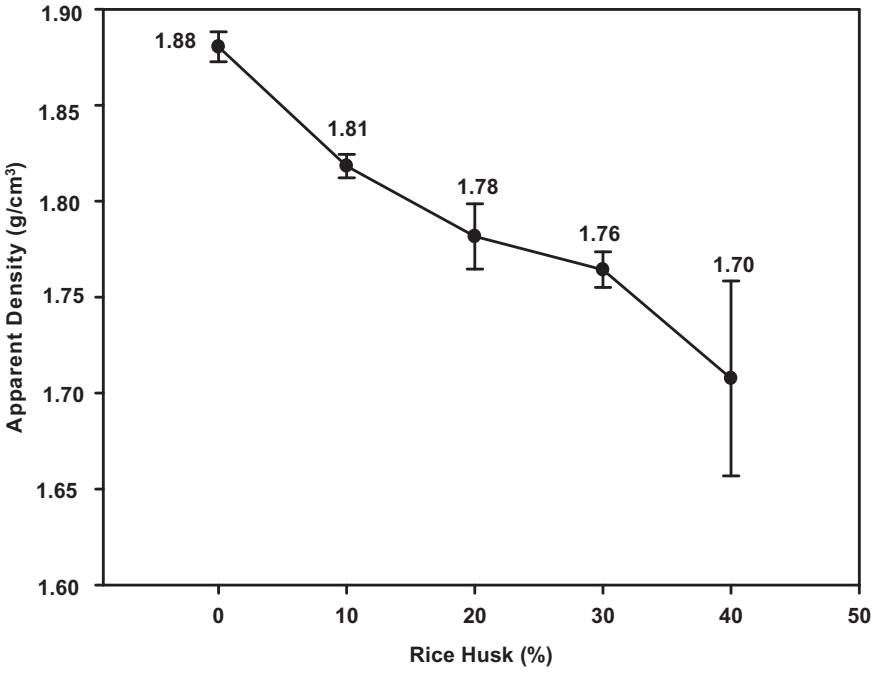

Figure 9. Apparent densities of geopolymer mortars as function of replacement level of metakaolin by rice husk.

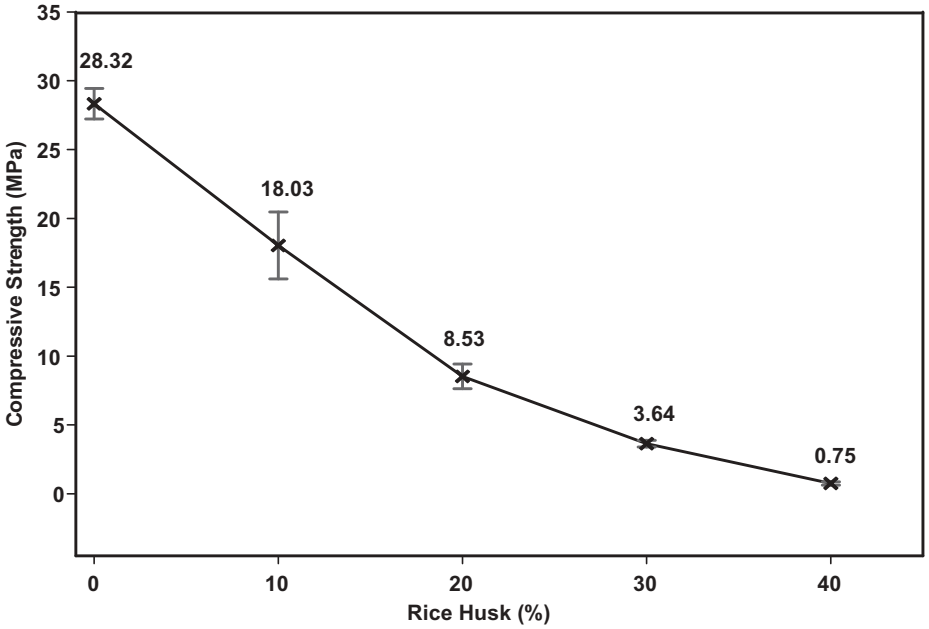

Figure 10. Compressive strengths of geopolymer mortars as function of replacement level of metakaolin by rice husk.

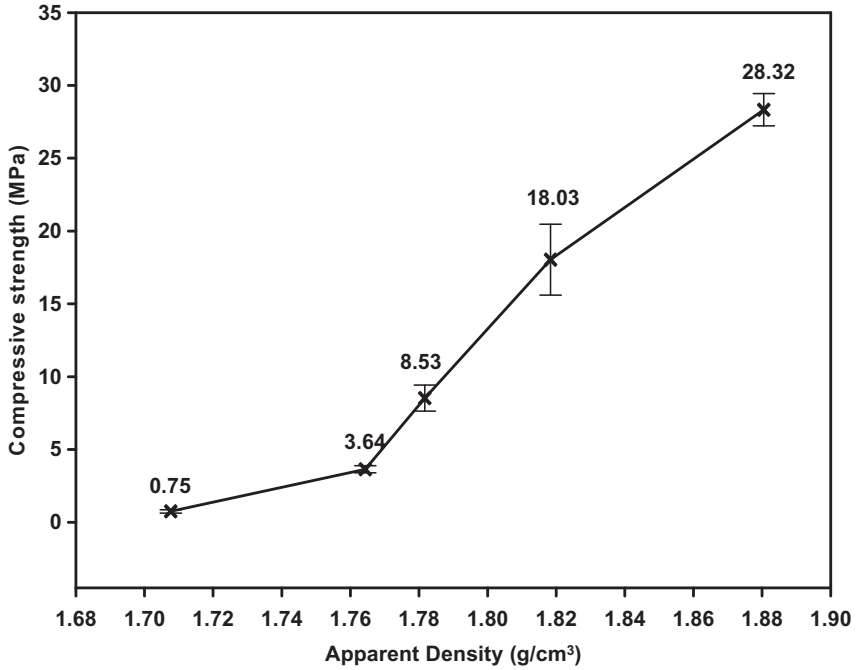

Figure 11. Compressive strengths of geopolymer mortars as function of apparent densities.

network. It is important to note that amorphous silica from RH are not included in the network owing to the large particles of rice husk that do not dissolve in the presence of sodium waterglass.

4.3.3. Optical microscope and scanning electron microscope (SEM)

Figure 12 depicts optical microscopic images of MGPC0, MGPC10, MGPC20, MGPC30 and MGPC40 geopolymer mortars. As can be seen, the optical microscope image of MGPC0 indicates that sand is embedded by the binder and that the structure is more compact, homogeneous and dense. This is in agreement with the higher value of the apparent density of the MGPC0 geopolymer mortar (1.88 g/cm^3). The optical microscopic images of the MGPC10, MGPC20, MGPC30 and MGPC40 geopolymer mortars clearly show some pores and particles of rice husk in the network, which increase with decreases in the values for the apparent density (Figure 9) and compressive strength (Figure 10). This figure clearly shows that the amount of binder decreases with increases in the amount of rice husk added leading to the formation of the sustainable lightweight geopolymer mortars.

Micrographic images of the MGPC0, MGPC20 and MGPC40 geopolymer mortars observed with different

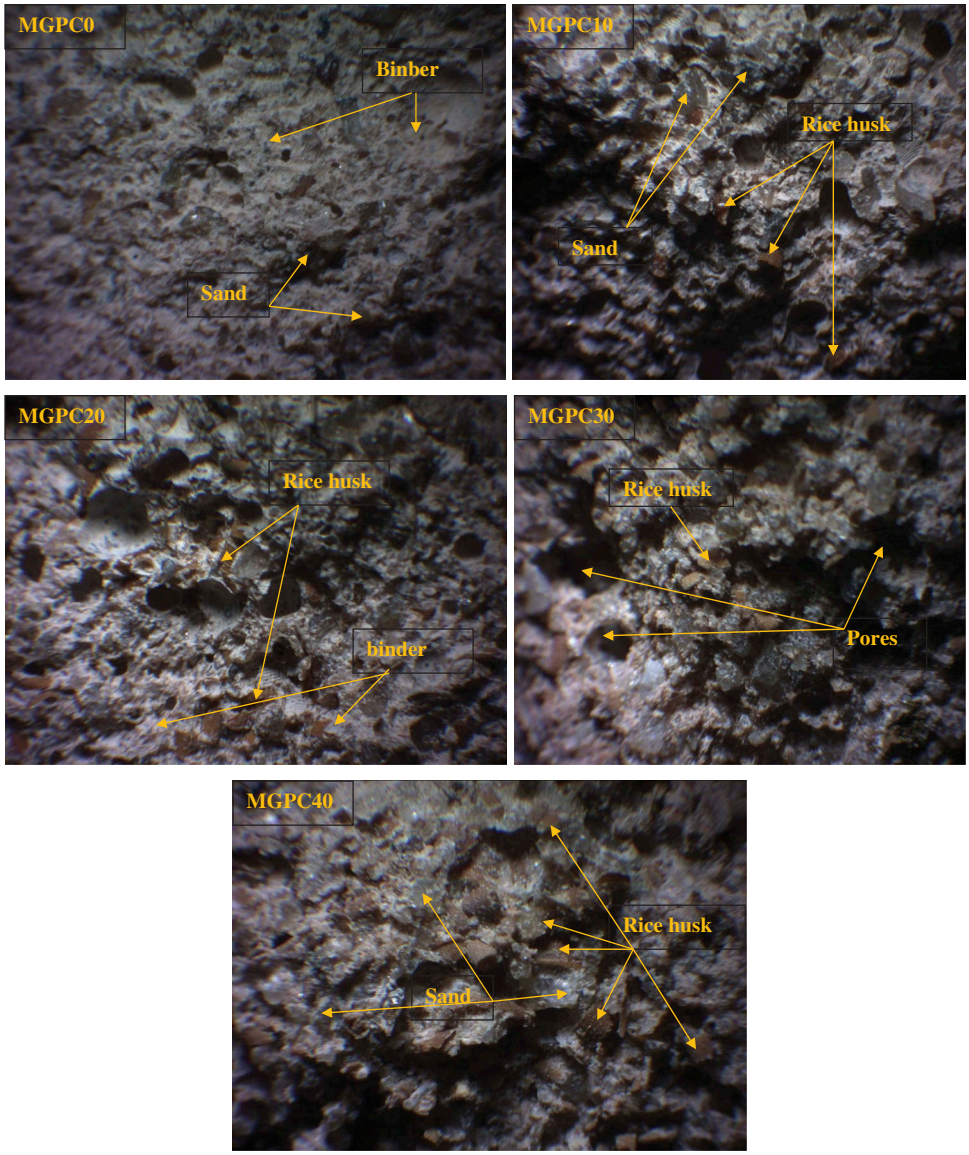

Figure 12. Optical microscope images of geopolymer mortars.

magnifications are presented in Figure 13. As can be seen, the micrographic images of MGPC0 show a dense and homogeneous microstructure owing to the formation of a compact binder. This indicates that the particles of poly(sialate-siloxo) are well interconnected with the sand. The denser matrix of MGPC0 geopolymer mortars is consistent with its higher value for the compressive strength (Figure 10) and apparent density (Figure 9). The micrographs of MGPC20 and MGPC40 observed with 100x magnification show some fine pores, whereas those of MGPC20 with 500x and 5000x magnification and the one of MGPC40 with 5000x magnification indicate a predominance of fibres rice husk. The micrographic image of MGPC40 with 500x magnification shows more large pores in its network. The presence of a large number of pores and fibres of RH is in agreement with the lower values for the apparent density (Figure 9) and compressive strength (Figure 9) and with the disappearance of the absorption band at about 728 cm^{-1} from its IR spectra (Figure 8).

4.3.4. Mercury intrusion porosimetry (MIP)

Figure 14 displays the results for the cumulative volume intrusion versus the pore size radius of the selected MGPC0, MGPC20 and MGPC40 geopolymer mortars. It appears that the cumulative volume intrusion of MGPC0, MGPC20 and MGPC40 are 116, 148 and 179.5 mm^3/g, respectively. It can be seen that the MGPC20 and MGPC40 geopolymer mortars contained a higher volume of pores in their networks compared to that of MGPC0. This is consistent with the values for the compressive strength and apparent density. The increase in the cumulative pore volume from 116 to 179.5 mm^3/g is related to a reduction of the binder in the geopolymer networks leading to the formation of more pores. The fine and large pore content of each selected specimen determined by mercury intrusion porosimetry shows that values for the fine pore content in MGPC0, MGPC20 and MGPC40 geopolymer mortars are 82.76, 67.23 and 34.26 %, respectively, while those for the large pore content are 17.24, 32.77 and 65.74 %,

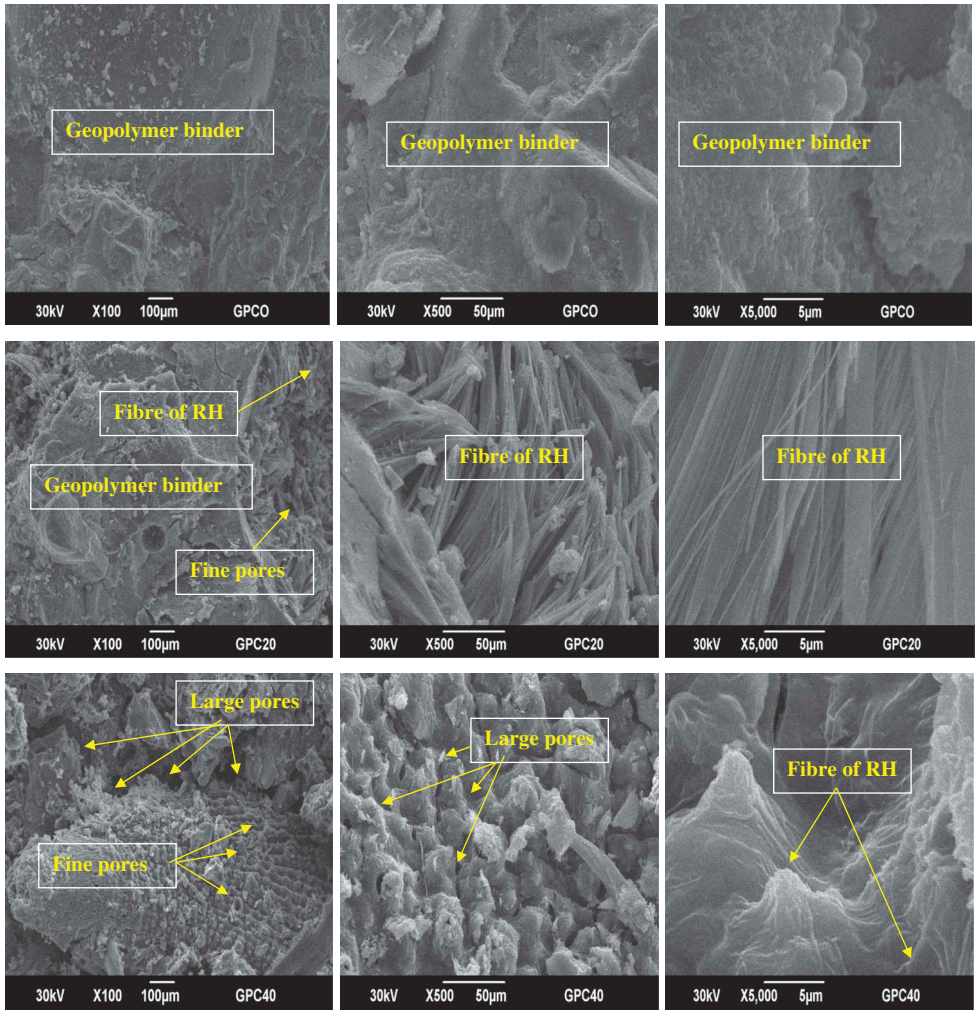

Figure 13. Micrograph images of geopolymer mortars MGPC0, MGPC20 and MGPC40.

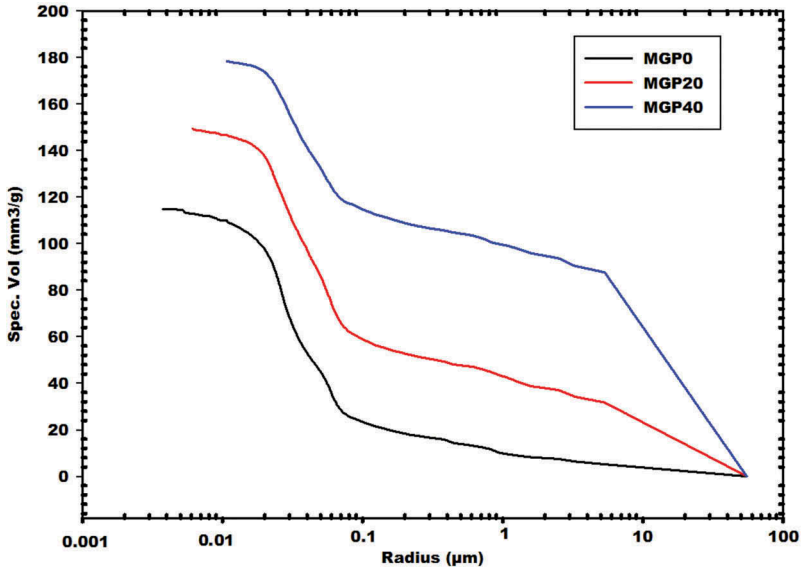

Figure 14. Cumulative pore volumes of geopolymer mortars, MGPC0, MGPC20 and MGPC40.

respectively. It appears that the fine pore content decreases and the large pore content increases with increases in the amount of rice husk added in the system. The increase in the large pore content is in agreement with the SEM images (Figure 11) of MGPC20 and MGPC40, which show more pores and more rice husk fibres in their structure. The large pore content in MGPC20 and MGPC40 corroborates the values for apparent density and compressive strength. The SEM and optical microscopic results suggest that rice husk is

appropriate for use in the preparation of lightweight geopolymer mortars.

5. Conclusion

Rice husk was used in this study as a natural foaming agent to conduct an in-depth investigation of the formation of pores in the structures of geopolymer mortars and cements. Metakaolin was substituted with 0, 10, 20, 30 and 40% by weight of rice husk. The resulting powders were used to synthesize lightweight geopolymer cements and mortars using sodium waterglass as a hardener. Rice husk and lightweight geopolymer cements were characterized by X-ray diffractometry and infrared spectroscopy. Lightweight geopolymer mortars were characterized by measuring the compressive strength, apparent density with mercury intrusion porosimetry and optical and scanning electron microscopy. The results show that rice husk consists mainly of amorphous silica and organic materials such as cellulose. The values for the compressive strength and apparent density of geopolymer mortars decrease and increase in cumulative volume as the ratio of rice husk incorporated in metakaolin increases. Stereomicroscopic and scanning electron microscopic images indicated the presence of rice husk, rice husk fibres and pores in the structure of geopolymer mortars. Infrared spectra of lightweight geopolymer cements showed the gradual disappearance of the absorption band at around 728 cm^{-1} attributable to sialate bonds, suggesting a decrease in the amount of binder in geopolymer cement when metakaolin was replaced with the proportions of rice husk employed in the study. It was found that a reduction of binder in the network leads to the formation of pores and therefore to the formation of lightweight geopolymer cements and mortars. Based on these properties, we can conclude that it is possible to use rice husk as an alternative foaming agent for the production of lightweight geopolymer cements, mortars and concretes.

Article highlights

- Rice husk was used as foaming agent for producing lightweight geopolymer mortars .
- The compressive strengths and apparent densities decrease with increasing the amount of rice husk.
- The reduction of the binder in the network leads to the formation of the pore.
- Rice husk an alternative foaming agent for the production of lightweight geopolymer concrete.

Acknowledgments

Hervé Tchakouté Kouamo gratefully acknowledges the Alexander von Humboldt Foundation for its financial support for this work under grant **N◦ KAM/1155741 GFHERMES-P**. The authors would also like to thank Mr Valerie Petrov for his SEM observations.

Disclosure statement

No potential conflict of interest was reported by the authors.

Funding

This work was supported by the Alexander von Humboldt-Stiftung [KAM/1155741 GFHERMES-P];

References

[1] Skvára F, Sulc R, Tišler Z, et al. Preparation and properties of fly ash-based geopolymer foams. Ceramics – Silikáty. 2014;58:188–197.
[2] Alghamdi H, Neithalath N. Novel synthesis of lightweight geopolymer matrices from fly ash through carbonate-based activation. Mater Today Commun. 2018;17:266–277.
[3] Ngouloure ZNM, Nait-Ali B, Zekeng S, et al. Recycled natural wastes in metakaolin-based porous geopolymers for insulating applications. J Build Eng. 2015;3:58–69.
[4] Fongang RTT, Pemndje J, Lemougna PN, et al. Cleaner production of the lightweight insulating composites: microstructure, pore network and thermal conductivity. Energy Build. 2015;107:113–122.
[5] Yahya Z, Razak RA, Al Bakri MM, et al. Rice husk (RH) as additive in fly ash base geopolymer mortar. Amer Inst Phys. 2017;1885:1–7.
[6] Tchakouté HK, Rüscher CH, Kong S, et al. Synthesis of sodium waterglass from white rice husk ash as an activator to produce metakaolin-based geopolymer cements. J Build Eng. 2016a;6:252–261.
[7] Tchakouté HK, Rüscher CH, Kong S, et al. Geopolymer binders from metakaolin using sodium waterglass from waste glass and rice husk ash as alternative activators: a comparative study. Constr Build Mater. 2016b;114:276–289.
[8] Tchakouté HK, Rüscher CH, Kong S, et al. Comparison of metakaolin-based geopolymer cements from commercial sodium waterglass and sodium waterglass from rice husk ash. J Sol-Gel Sci Technol. 2016c;78:492–506.
[9] Kamseu E, À Moungam LMB, Cannio M, et al. Substitution of sodium silicate with rice husk ash-NaOH solution in metakaolin-based geopolymer cement concerning reduction in global warming. J Cleaner Prod. 2017;142:3050–3060.
[10] Melele SJK, Tchakouté HK, Banenzoué C, et al. Improvement of the reactivity of soda lime silica glass solution as a hardener for producing geopolymer materials. Bull Mater Sci. Manuscript submitted.
[11] Mabah DET, Tchakouté HK, Rüscher CH, et al. Design of low cost semi-crystalline calcium silicate from biomass for the improvement of the mechanical and microstructural properties of metakaolin-based geopolymer cements. Mater Chem Phys. 2019;223:98–108.
[12] Tchuenté FM, Tchakouté HK, Banenzoué C, et al. Microstructural and mechanical properties of (Ca, Na)-poly(sialate-siloxo) from metakaolin as aluminosilicate

and calcium silicate from precipitated silica and calcined chicken eggshell. Constr Build Mater. 2019;201:662–675.
[13] Ngwa CA. Development authorities as agents of socio-economic change: a historical assessment of the upper nun valley development authority (UNVDA) in the Ndop region of Cameroon, 1970–1995. Nordic J Afr Stud. 2019;12:220–237.
[14] Fonjong LN, Athanasia MF. The fortunes and misfortunes of women rice producers in Ndop, Cameroon and the implications for gender roles. J Inter Women's Stud. 2007;8:133–147.
[15] Nzembayie MJ, Melo N. Agricultural decline and the need for sustainable tourism alternatives in Ndop Central Sub-Division, North West Cameroon. J Agric Res Developm. 2015;5:145–155.
[16] Ngon Ngon GF, Etame J, Ntamak-Nida MJ, et al. Geological study of sedimentary clayey materials of the Bomkoul area in the Douala region (Douala subbasin, Cameroon) for the ceramic industry. C R Geosci. 2012;344:366–376.
[17] Bukalo NN Paleoenvironmental reconstruction of cretaceous-tertiary kaolin deposits in the Douala subbasin in Cameroon. PhD Thesis. University of Venda, South Africa, 2017, pp. 389.
[18] Liu J, Yao Y, Liu D, et al. Experimental simulation of the hydraulic fracture propagation in anthracite coal reservoir in the southern Qinshui Basin, China. J Pet Sci Eng. 2018;168:400–408.
[19] Tchakouté HK, Rüscher CH, Djobo JNY, et al. Influence of gibbsite and quartz in kaolin on the properties of metakaolin-based geopolymer cements. Appl Clay Sci. 2015;107:188–194.
[20] Keiluweit M, Nico PS, Johnson MG, et al. Dynamic molecular structure of plant biomass-derived black carbon (biochar). Environ Sci Technol. 2010;44:1247–1253.
[21] Al- Wabel MI, Al-Omran A, El-Nagar AH, et al. Pyrolysis temperature-induced changes in characteristics and chemical composition of biochar produced from Conocarpus wastes. Bioresour Technol. 2013;131:374–379.
[22] Nakbanpote W, Goodman BA, Thiravetyan P. Copper adsorption on rice husk derived materials studies by EPR and FTIR. Colloids Surf A Physicochem Eng Asp. 2007;304:7–13.
[23] Rees CA, Provis JL, Lukey GC, et al. In situ ATR-FTIR study of the early stages of fly ash geopolymer gel formation. Langmuir. 2007;23:9076–9082.
[24] Shi J, Xing D, Li J. FTIR studies of the changes in wood chemistry from wood forming tissue under inclined treatment. Energy Procedia. 2012;16:758–762.
[25] Emdadi Z, Asim N, Yarmo MA, et al. Effect of chemical treatments on rice husk (RH) water absorption property. Inter J Chem Eng Appl. 2015;6:273–276.
[26] Brewer CE, Schmidt-Rohr K, Satrio JA, et al. Characterisation of biochar from fast pyrolysis and gasification systems. Environ Prog Sustain Energy. 2009;28:386–396.
[27] Kim KH, Kim JY, Cho TS, et al. Influence of pyrolysis temperature on physiochemical properties of biochar obtained from the fast pyrolysis of pitch pine (Pinusrigida). Bioresour Technol. 2012;118:158–162.
[28] Wang L, Liu L, Holmes J, et al. Assessment of film-forming potential and properties of protein and polysaccharide-based biopolymer films. Int J Food Sci Technol. 2007;42:1128–1138.
[29] Le Traèdec M, Peyratout C. Physico-chemical modifications of the interactions of the interactions between hemp fibres and a lime mineral matrix: impact on mechanical properties of mortars. Proceeding of 10th European Ceramic Society; 2007; p. 451–456.
[30] Sugashini S, Begum KMMS. Performance of ozone-treated rice husk carbon (OTRHC) for continuous adsorption of Cr(VI) ions from the synthetic effluent. J Environ Chem Eng. 2013;1:79–85.
[31] Bardalai M, Mahanta DK. Characterization of rice husk through X-ray diffraction, scanning electron microscope and Fourier transforms infrared analysis. Inter J Innov Res Sci Eng. 2016;2:472–479.
[32] Tchakouté HK, Rüscher CH, Kong S, et al. Thermal behavior of metakaolin-based geopolymer cements using sodium waterglass from rice husk ash and waste glass as alternative activators. Waste Biomass Valorization. 2017;8:573–584.
[33] Bewa CN, Tchakouté HK, Fotio D, et al. Water resistance and thermal behavior of metakaolin-phosphate-based geopolymer cements. J Asian Ceram Soc. 2018;6:271–283.
[34] Rüscher CH, Mielcarek EM, Wongpa J, et al. Silicate-aluminosilicate and calcium silicate gels for building materials: chemical and mechanical properties during ageing. Eur J Mineral. 2011;23:111–124.
[35] Melele SJK, Tchakouté HK, Banenzoué C, et al. Investigation of the relationship between the condensed structure and the chemically bonded water content in the poly(sialate-siloxo) network. Appl Clay Sci. 2018;156:77–86.
[36] Hassan HS, Abdel-Gawwad HA, Vásquez García SR, et al. Fabrication and characterization of thermally-insulating coconut ash-based geopolymer foam. Waste Manage. 2018;80:235–240.